Voltage stability margin determination using the channel components transform

DOI:
10.1109/PTC.2015.7232661

Document status and date:
Published: 31/08/2015

Document Version:
Accepted manuscript including changes made at the peer-review stage

Voltage Stability Margin Determination Using the Channel Components Transform

Jhon A. Castrillon, Juan S. Giraldo and Carlos A. Castro
University of Campinas (UNICAMP)
Campinas, Brazil
jacastri@dsee.fee.unicamp.br, j.s.g@ieee.org, ccastro@ieee.org

***Abstract*—This paper shows that the voltage stability margin of a power network can be determined through the application of a transformation that allows the decomposition of the grid into a set of decoupled source-line-load circuits. By monitoring a small number of these circuits one can analyze the behavior of the actual power system. Therefore it is not necessary to monitor the complete network, since by observing this particular circuit group one can determine the voltage stability conditions of the actual grid, which is of great interest for the real time operation.**

***Index Terms*—Channel Components Transform, Load Scaling Factor, Voltage Stability Margin.**

I. Introduction

Many blackouts in recent years have been caused by power network instabilities, so stability had become a crucial aspect for the power network secure operation. Voltage instability events have happened after several recent disturbances in power systems around the world and a significant research effort has been performed in order to deal with it [3]. The blackout that took place in the northeast coast of the USA and Canada on August 2003 [1], the other ones that happened in Europe soon after and the blackout of great proportions in Brazil in 2009 are some recent examples of the severe consequences of instabilities in a power system.

The increased number of interconnections, the use of new technologies and control devices, the operation under stressed conditions due to consistent load increase, especially at peak hours, as well as the difficulties to supply the loads and the operation of equipment close to their limits led systems to become susceptible to instability problems, such as voltage instability, frequency instability and inter area oscillations [2]. In addition, the power transfers between companies and the environmental and resource restrictions for the expansion and reinforcement of the networks have also led to a growing concern about operation security of the power systems, mainly on voltage stability.

Although this issue is not new, there are still difficulties about the correct monitoring and control by the utilities. Therefore, there is still a need to develop methodologies and procedures that can be applied to maintain the operating state of the system into balance.

In this paper the main interest is on including voltage stability analysis as a fundamental item in the security analysis, mostly in real time operation and the operation planning. Obtaining the voltage stability conditions of the power networks with a low computational effort is of great interest for real time operation, since it would represent an improvement on the efficiency of the procedure in comparison to conventional methods such as the ones based on the analysis of the Jacobian matrix [4]. The method proposed in this paper consists on the application of a transformation that allows the analysis of the power system through simple two-bus circuits.

The remaining of this paper is organized as follows. Section II presents the main aspects of the proposed transform. In section III the proposed transform is used and a method is presented to obtain the voltage stability margin of a power system. Section IV shows some test results for IEEE power networks under different load conditions. Finally, Section V contains the main conclusion of this work.

II. Channel components transform (CCT)

The power network can be represented as a multinode, multibranch Thevenin equivalent circuit connecting loads to generators. The aim of the CCT is to perform the eigen-decomposition on the Thevenin impedance matrix for converting a complex network into a set of decoupled circuits named channels. By the analysis of these circuits it is possible to obtain important information about the behavior of the actual network. This modal decomposition has been used extensively in linear system analysis [5]-[6].

It is shown in [7] the Thevenin equivalent circuit representation of a generic power system and how the Thevenin impedance matrix $[Z]$ and matrix $[K]$ are handled from the network topology matrix represented in a specific order. By performing the modal decomposition on the $[Z]$ matrix, one has

This work was supported by Brazilian funding agencies FAPESP, CAPES and CNPq.

$$[Z] = [T]^{-1}[\lambda][T]\ , \quad (1)$$

where $[\lambda]$ e $[T]$ are the eigenvalue and eigenvector matrices of $[Z]$, respectively. By substituting (1) into the equation of the Thevenin equivalent circuit model [7], it is possible to observe how the network is decoupled, as follows.

$$[T][V] = [T][K][E] - [\lambda][T][I]\ , \quad (2)$$

where vectors $[V]$, $[I]$ and $[E]$ correspond to load voltages, load currents and generator voltages, respectively. Denoting $[U] = [T][V]$ as the transformed voltage, $[J] = [T][I]$ as the transformed current and $[F] = [T][K][E]$ as the transformed voltage source, (2) can be rewritten as

$$\begin{bmatrix} U_1 \\ U_2 \\ \cdots \\ U_n \end{bmatrix} = \begin{bmatrix} F_1 \\ F_2 \\ \cdots \\ F_n \end{bmatrix} - \begin{bmatrix} \lambda_1 & 0 & 0 & 0 \\ 0 & \lambda_2 & 0 & 0 \\ 0 & 0 & . & 0 \\ 0 & 0 & 0 & \lambda_n \end{bmatrix} \begin{bmatrix} J_1 \\ J_2 \\ \cdots \\ J_n \end{bmatrix}. \quad (3)$$

This transform allows the decomposition of a power network with n loads into a set of n decoupled source-line-load channels that represent virtual power flow paths as shown in Fig. 1.

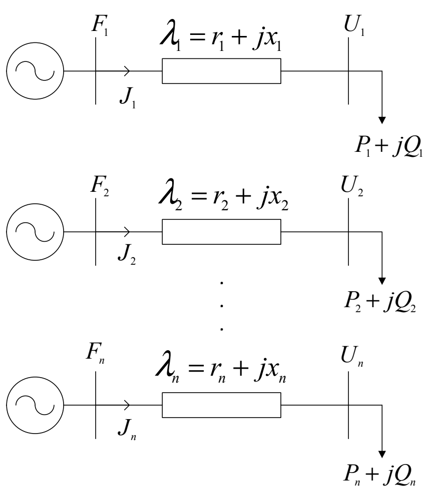

Fig. 1. Channel representation of a power network (adapted from [7]).

Once the transformation is performed the channel loads become coupled, as discussed in [7]. As a result, the channels' operating points might go beyond the nose point of the respective channel PV curve, while the actual system is still stable. For that reason it is necessary to find a way to represent these coupling effects independently from the loads. Since each channel load contains $[F]$ and $[\lambda]$ components associated with the other channels, it is possible to model the load coupling through a Norton current source, as shown in Fig. 2. According to [7] the current injection for each channel is determined from

$$JE_i = J_i - Y_{Cii}U_i\text{, and} \quad (4)$$

$$[Z_C] = [T][Z_L][T]^{-1}, \quad (5)$$

where Y_{Cii} corresponds to the diagonal element of the inverse matrix of $[Z_C]$ and $[Z_L]$ is the physical load impedances, which is a diagonal matrix.

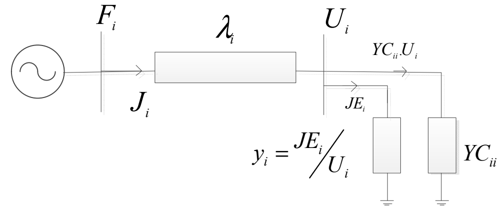

Fig. 2. Channel circuit *i* with the current source injection.

Differently from [7], for our purpose the analysis is performed using an association of the two admittances shown in Fig. 2, resulting in the channel circuit as shown in Fig. 3.

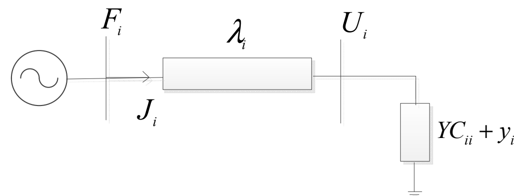

Fig. 3. The i^{th} channel circuit taking the load coupling into account.

The key advantage of representing the grid through channels is the small effort required for analyzing its behavior through the more representative channels for the power transfer. This transformation was named *CCT* to differentiate from other known kinds of transformations, as for example, the several modal transformations [7].

III. Voltage Stability Margin

Operate the system close to the transmitted power limit is very risky, since a small disturbance such as a light load increase would lead the network to the voltage collapse. Therefore, the estimation of the security margin from the current operational point to the maximum loading point is an important factor for the system security.

A. Maximum Loading Factor of the Channels (MLFC)

One particularly interesting aspect about *CCT* is the possibility of determining the loading margin in each individual channel analytically, in a simple way. Since the power network can be represented as a set of simple two-bus circuits, one can obtain an expression that shows the relationship between the transformed voltage (U) and the transformed load power consumption (P and Q) for each channel. Considering channel *i* shown in Fig.3 as an example, it is possible to derive the following equation.

$$U_i^{\ 4} + \left[2a\Lambda_i - F_i^{\ 2}\right]U_i^{\ 2} + \Lambda_i^{\ 2}[a^2 + b^2] = 0\ , \quad (6)$$

where $a = (r_iP_i + x_iQ_i)$ and $b = (r_iQ_i - x_iP_i)$. Variable Λ_i is a parameter that scales the load, assuming that it changes with constant power factor. r_i and x_i are respectively the real and imaginary parts of λ_i.

From (6) it is possible to obtain the PV curve for each channel and confirm that each one of them carries a different amount of power [8]. The maximum transformed power S_{max} for channel *i* is calculated as

$$|S_{max}| = \frac{|F_i|^2[|\lambda_i| - (x_i \sin\theta_i + r_i \cos\theta_i)]}{2[x_i \cos\theta_i - r_i \sin\theta_i]^2}, \qquad (7)$$

where θ_i is the power factor angle of the load of the i^{th} channel.

The maximum loading factor of each channel taking into account the load coupling effect is obtained as follows.

Step 1: Obtain S_{max}, which is the maximum power consumption at the load in the equivalent circuit (Fig. 3 and (7)).

Step 2: Calculate $|U_i'|^2 = S_{max}/(YC_{ii} + y_i)^*$, where U_i' corresponds to the load voltage at the respective maximum power consumption.

Step 3: Calculate $S'_{max} = |U_i'|^2 \cdot (YC_{ii})^*$, which is the power consumption corresponding exclusively to the individual channel (load coupling is disregarded at this point).

Due to the variation of the current injection JE_i with the other channel voltages, the procedure above is necessary for the stability margin calculation, where S'_{max} is the maximum power related to component YC_{ii} (Fig. 2). Therefore, the maximum loading factor for the i^{th} channel *(MLFC)* is

$$\Lambda_i^* = \frac{|S'_{max}|}{||U_i|^2 \cdot (YC_{ii})^*|}. \qquad (8)$$

The values that Λ_i^* can take for the different channels provide important information about the voltage stability condition of the actual network.

B. Maximum Loading Point (MLP) using Load Flow with Step Size Optimization (LFSSO).

Conventional load flow methods present convergence problems for ill-conditioned systems, even for feasible operating points, which is not a desirable situation. In order to overcome this difficulty several approaches have been proposed. Moreover, it is expected that a load flow method be able to provide additional information about the iterative process so that the voltage stability analysis method can take advantage of it. It is the case of the method proposed in [9], where the step size optimization factor (μ) assumes values around unity for feasible operating points and tends to zero for infeasible ones, indicating whether they are within or without the feasible region, which is separated from the infeasible region by boundary surface Σ. In general terms, it is based on a conventional Newton-Raphson power flow, with a system of nonlinear equations $g(x, \rho)$, where x is the vector of system state variables (V, θ) and ρ the load scale factor used to modify the generation and load. The state variables at the τth iteration are

$$x^{(\tau+1)} = x^{(\tau)} + \mu^{(\tau)} \Delta x^{(\tau)}. \qquad (9)$$

Assuming an initial point in the infeasible region ($\rho^0 > \rho^{mlp}$), *LFSSO* converges to the point MLP^0 on the feasibility boundary, as shown in Fig. 4.

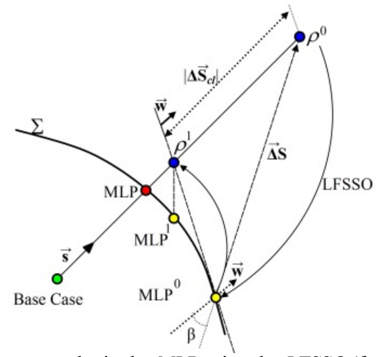

Fig. 4. Process to obtain the *MLP* using the *LFSSO* (from[10]).

According to [11], unit vector $\vec{w}$, normal to boundary Σ at *MLP* is computed and identified in Fig. 4 as MLP^0. Then, a normal plane, which is at the same time tangent to MLP^0, intersects with the load increase direction $\vec{S}$ is computed. The intersection point determines the updated loading factor (ρ^1) and the load curtailment $|\Delta\vec{S}_{cl}|$ that must be performed. Therefore, the loading factor correction $\Delta\rho$ can be calculated as

$$\Delta\rho = |\Delta\vec{S}_{cl}|/|\vec{S}| = (\Delta\vec{S} \cdot \vec{w})/(\vec{S} \cdot \vec{w}), \qquad (10)$$

where $\Delta\vec{S}$ is the power difference between MLP^0 and the power value with $\rho = \rho^0$ in this case, and $\vec{w}$ can be calculated from (11) knowing that $\nabla_x g(x_{mlp})$ is the Jacobian matrix of g evaluated at MLP^0.

$$\nabla_x g(x_{mlp})^T \vec{w} = 0 \cdot \qquad (11)$$

This procedure must be performed until the actual *MLP* is reached using the updated values of MLP^τ and ρ^τ for later iterations. The method in [10] also includes an acceptable error $\pm x\%$ in the computation of the *MLP*, that is, the operator is willing to accept an error of $\pm x\%$ in the computed voltage stability margin. This acceptable error results in an ideally acceptable margin within a fixed width. Parameter α represents this width and is defined as

$$\alpha = (1 + x/100)/(1 - x/100) \cdot \qquad (12)$$

The *MLP*, identified as ρ^{mlp}, can be calculated as detailed below.

1) Set counter i =0. Set ρ^i.
2) Run *LFSSO* for ρ^i. If $\mu \to 0$ go to 3). Else, $\rho_{temp} = \rho^i$ and go to 5).
3) Obtain $\rho_{temp} = 1$ and go to 4).
4) Run *LFSSO* for ρ_{temp}. If $\mu > 0$ continue. Else, go 6).
5) Run *LFSSO* for $\rho^{i+1} = \alpha\rho_{temp}$. If $\mu \to 0$ then $\rho^{\wedge mlp} = (\rho_{temp} + \rho^{i+1})/2$, then End. Else, $\rho^{i+1} = (\rho^i + \rho^{i+1})/2$, do i=i+1 then go to 2).
6) Run *LFSSO* for $\rho^{i+1} = \alpha/\rho_{temp}$. If $\mu > 0$ $\rho^{\wedge mlp} = (\rho_{temp} + \rho^{i+1})/2$ then End. Else, i=i+1 and go to 3).

C. *Voltage Stability Determination using CCT.*

Among the different resulting channels there is one which its *MLFC* follows the actual network´s maximum loading factor at any loading condition, as shown in Fig. 5, allowing the estimation of an estimated margin behavior. Fig. 5 shows the load demand curve for a 24 hour period, the corresponding voltage stability margin and the margins computed for each channel (*MLFC*). For illustration purposes, the IEEE 57-bus system was used in this simulation. Since the *LFSSO* determines de *MLP* in a power system, one can use the *MLFC* from this channel as an initial point for the voltage stability margin determination.

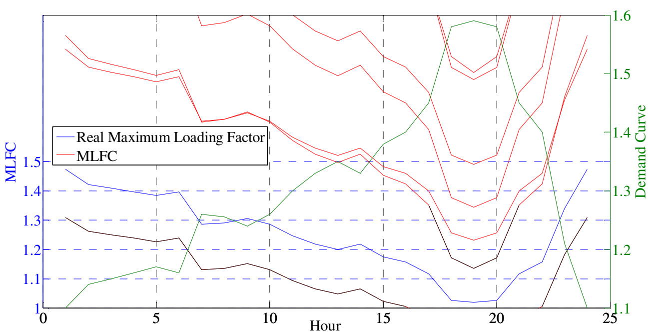

Fig. 5. Some *MLFC* from *IEEE 57-bus system*.

Fig. 5 shows that the *MLFC* for some channels of the *IEEE 57-bus system*, where it is possible to note, that there is one channel (black line) that follows the real network loading. According to the daily demand curve this channel can change. For example, note that the channel of interest for hours 17 to 21 is different from the one from hours 0 to 17 and for hours 22 to 24. The small number of critical channels is of great interest for real time operation because a small number of channels is necessary for monitoring the system.

For the channel identification and actual margin calculation the algorithm is proposed next.

1) For first time instant under analysis, compute the average of the maximum loadings from the first *MLFC* that falls into the interval 1 to 2. Set ρ^i to this value.

2) Run the *LFSSO* and obtain the *MLP*.

3) Calculate the voltage stability margin of the actual network as $SM = (MLP^i - 1).100\%$.

4) For the next time instant, find the *MLFC* closer to *MLP* and go to *2).*

$$\rho^{i+1} = MLFC\ (min|MLFC_{i+1} - MLP|)$$

For actual systems loadings larger than twice the base case are not common. For that reason, step 1) of the procedure above considers the average over this range in order to locate the first estimation for the channel. Fig. 6 shows the process of voltage stability margin determination using the *CCT*.

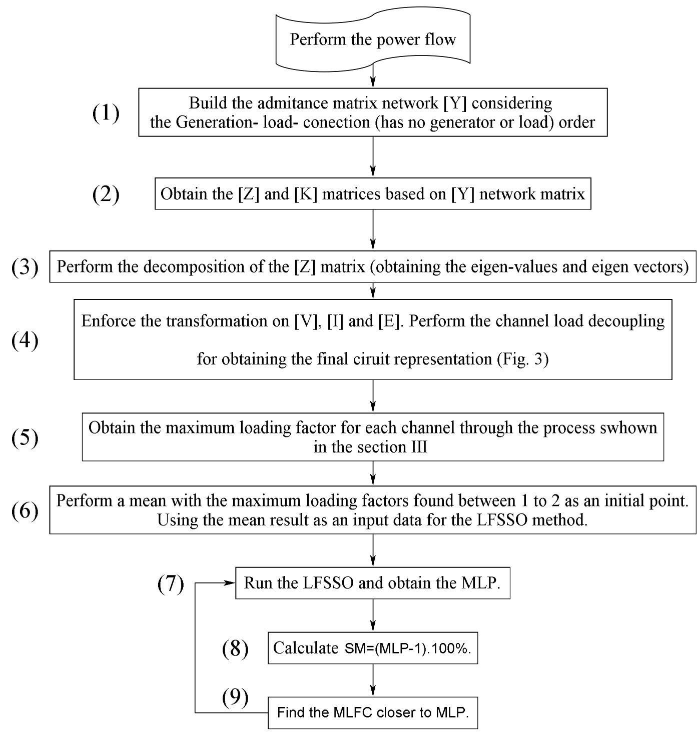

Fig. 6. Flowchart for voltage stability margin determination.

The flowchart shown in Fig. 6 is appropriate for offline analysis, where the input data are obtained from performing power flows. For online applications each operating point can be obtained from synchronized phasor data [13] and/or state estimation [14]. The *CCT* must be performed for each loading condition. Other analysis can be performed with the aid of this transformation, as the determination of the critical buses, generators and branches [15].

IV. Test Results

The proposed method was tested for IEEE 14, 57, 118 and 300 bus systems in order to obtain the maximum loading factor and consequently the voltage stability margin of an actual power network. All loads and generators were scaled by a same factor in order to simulate the daily demand variation; each system was driven relatively near to its *MLP*.

Simple Case Study

From a simple five bus system in [7] and equation (11) it is possible to obtain the PV curve for the channels and verify that each one carries a different amount of power. The network of Fig. 7 has the following parameters in per unit: $Z_a = 0.35j$, $Z_b = 0.2j$, $Z_c = 0.1j, Z = 0.3j, E = 1.0$, $S_3 = 0.3, S_4 = 0.25$ and $S_5 = 0.4$.

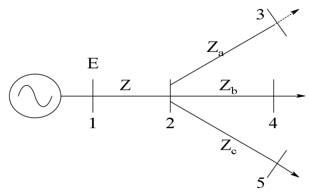

Fig. 7. Simple five bus network from [7].

As the network has three loads, the application of the *CCT* will result in three channels. Since the PV curves are one way to observe the proximity between the operating power and the maximum power (nose point), in this case they are obtained for each channel. After the decomposition with the application of the *CCT* and with aid of (11), the PV curve for the first channel is shown in Fig. 8.

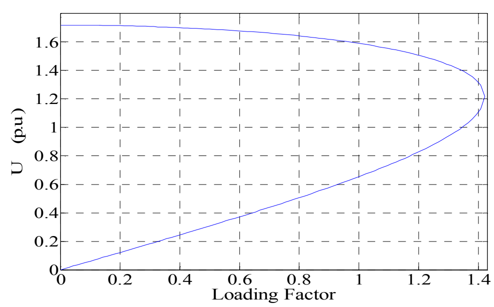

Fig. 8. *PV* Curve for the first channel of the simple case.

By performing successive power flows as shown in [16] it is possible to plot the PV curve for the actual network, as shown in Fig. 9. One can note that the maximum loading factor of this channel is close to the actual network's nose point, therefore one can infer that by just knowing the maximum loading factor of the critical channel it is possible to determine the voltage stability margin of the actual network. However, this is not always true, either due to the channels' precision or due to the channel' inability to take into account the reactive power limits of generators. For that reason it is necessary to make use of the *LFSSO*.

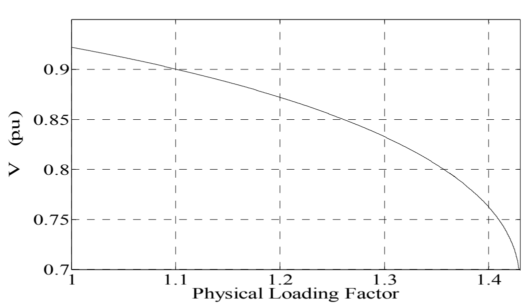

Fig. 9. *PV* Curve for the actual network.

IEEE Systems

In this case a daily demand curve is considered to calculate the maximum loading factor and to observe the behavior of the channel of interest in different load periods for the *IEEE* 57 bus system. Fig. 10 shows a comparison between the information provided by the *CCT-LFSSO* and the one resulting from performing multiple power flows as a reference, in order to verify the precision of the proposed method.

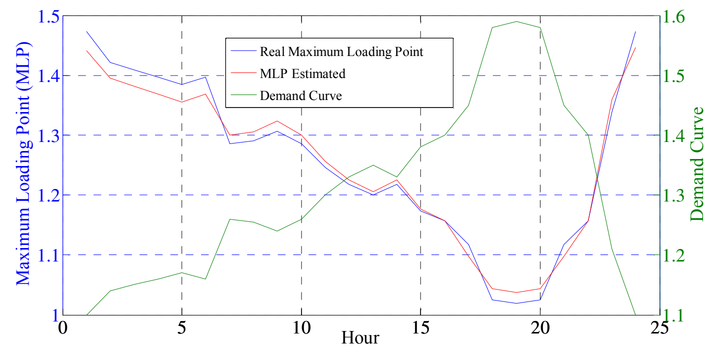

Fig. 10. Maximum loading point using *CCT* for the *IEEE* 57 bus system.

Fig. 5 shows that under different operating conditions during the day the channel that follows the real maximum loading point presents a considerable difference, but by using of the *MLFC* as an initial point to *LFSSO* the estimation of the *MLP* of the actual network is accurate, as shown in Fig. 10, where it is possible to observe the good precision when the estimated *MLP* (red line) is compared with the real maximum loading point of the actual network. Since the *MLFC* remains in a feasible region close to the actual value, the use of an inefficient initial point for the *LFFSO* is avoided, which is of great interest in real time operation.

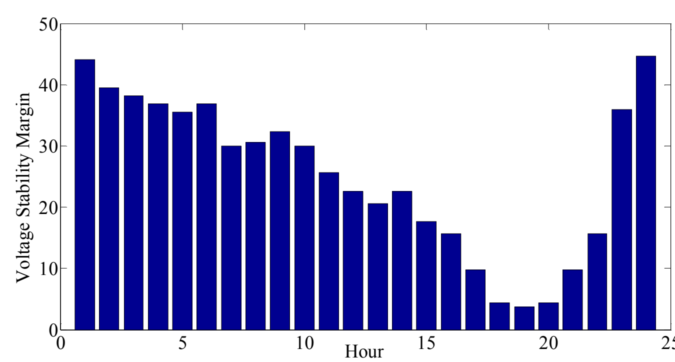

Fig. 11. Voltage stability margin for the *IEEE* 57 bus system.

Fig.11 contains the voltage stability margin calculated for each *MLP* from Fig. 10 according to the equation shown in the block (8) of the flowchart. The lowest margin occurs at hour 19 as it was expected (demand peak) and corresponds to 3.72%.

Fig. 12 has the purpose to show why the *MLFC* is important in the maximum loading point calculation and consequently voltage stability margin determination. Since the

MLFC is used as an initial point in the LFFSO one can observe that this factor is an excellent initializing point, because of its proximity to the actual *MLP*. Through the comparison between Fig. 12 and Fig. 5 is possible to observe that the *MLFC* for the channel of interest follows the actual value in spite of changing during a loading condition, which is an important advantage, because, it is just necessary to monitor a small number of channels for identifying the channel of interest and consequently the voltage stability margin determination of the network.

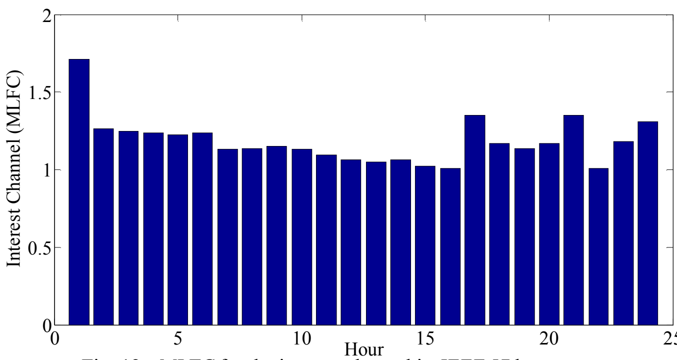

Fig. 12. *MLFC* for the interest channel in *IEEE* 57 bus system.

The voltage stability margin for the *IEEE* 300 bus system is also obtained and compared with the actual margin network as shown in Fig. 13.

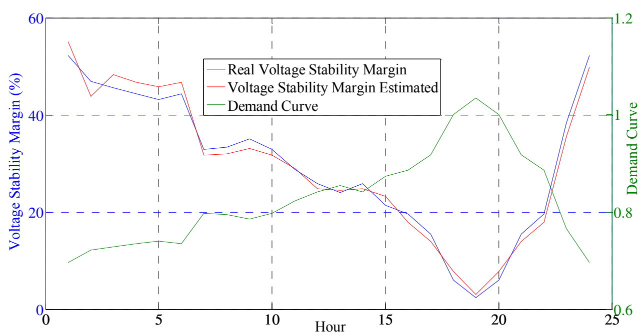

Fig. 13. Voltage stability margin for the *IEEE* 300 bus system.

It is possible to note that for both maximum loading points as the voltage stability margins, the proposed method works well at any loading condition, allowing the estimate of the network behavior from security point of view.

Table I shows the *MLP* for several IEEE system. The number of *LFSSO* iterations is smaller than commonly obtained in the continuation power flow. Note that the results obtained show that the proposed method has a good potential of being used in on-line, real time environments.

V. Conclusion

With the channel based voltage stability margin calculation, it is possible to find and identify one channel, which is located in the neighborhood of the actual maximum loading point. This fact allows monitoring and analyzing the voltage stability of the network in a very simple way, since it is only necessary to observe a small number of channels during the day which carry the most important information about the power transfer of the network. This is of great interest in real time operation.

Table I. *MLP* for base cases

System	Actual MLP	Proposed Method	Number Iterations$^{(*)}$
IEEE 14	1.7830	1.7916	7
IEEE 57	1.6170	1.6281	4
IEEE 118	2.1436	2.1738	13

$^{(*)}\, x = 2\%$.

References

[1] U.S.-Canada Power System Outage Task Force. Final Report on the August 14, 2003 Blackout in the United States and Canada: Causes and Recommendations, 2004. [available in https://reports.energy.gov/].
[2] P. Kundur et al. Definition and Classification of Power System Stability, IEEE Trans. Power Syst., vol. 19, n. 2, May 2004.
[3] Proceedings of the Bulk Power System Voltage Phenomena – III Seminar on Voltage Stability, Security & Control, ECC/NSF Workshop, Davos, Switzerland, 1994.
[4] V. Ajjarapu, C.Christy. The continuation power flow: a tool for steady state voltage stability analysis, IEEE Trans. Power Syst., vol. 7, n. 1, 1992.
[5] Gamm, A. Z., Golub, I. I., Bachry, A., & Styczynski, Z. A. Solving several problems of power systems using spectral and singular analyses. Power Systems, IEEE Transactions on, 20(1), 138-148, 2005.
[6] Gao, B., Morison, G. K., & Kundur, P. Voltage stability evaluation using modal analysis. Power Systems, IEEE Transactions on, 7(4), 1529-1542, 1992.
[7] W. Xu, I.R. Pordanjani, Y. Wang, E. Vaahedi. A Network Decoupling Transform for Phasor Data Based Voltage Stability Analysis and Monitoring, IEEE Trans. Smart Grid, vol. 3, n. 1, 2012.
[8] I.R. Pordanjani, Y. Wang, W. Xu. A Transformation Technique for Decoupling Power Networks, IEEE EPEC, 2011.
[9] Braz, L. M., Castro, C. A., & Murati, C. A. F, A critical evaluation of step size optimization based load flow methods. Power Systems, IEEE Transactions on, 15(1), 202-207, 2000.
[10] Xavier, C. E., Bedriñana, M. F., & Castro, C. A. Robust computation of voltage stability margins for transmission and distribution grids. In Power and Energy Society General Meeting (PES), (pp. 1-5). IEEE, 2013.
[11] Bedriñana, M. F., & Castro, C. A. Maximum loading point computation based on load flow with step size optimization. In Power and Energy Society General Meeting-Conversion and Delivery of Electrical Energy in the 21st Century, (pp. 1-8). IEEE, 2008.
[12] B. L. Tavares, M. F. Bedriñana, and C. A. Castro, "Practical method for computing the maximum loading point based on load flow with step size optimization," in Power and Energy Society General Meeting, IEEE, 2010, pp. 1–8.
[13] Phadke, A. G. Synchronized phasor measurements in power systems. Computer Applications in Power, IEEE, 6(2), 10-15, 1993.
[14] Chakrabarti, S., et al. "Inclusion of PMU current phasor measurements in a power system state estimator." IET generation, transmission & distribution 4.10:1104-1115, 2010.
[15] Pordanjani, I. R., Wang, Y., & Xu, W. Identification of critical components for voltage stability assessment using channel components transform. Smart Grid, IEEE Transactions on, 4(2), 1122-1132, 2013.
[16] V. Ajjarapu, C.Christy. The continuation power flow: a tool for steady state voltage stability analysis, IEEE Trans. Power Syst., vol. 7, n. 1, 1992.